Studies on Model Electrorheological Fluids

James W. Goodwin,* Gavin M. Markham, and Brian Vincent

School of Chemistry, University of Bristol, Cantock's Close, Bristol BS8 1TS, U.K.

Received: July 26, 1996; In Final Form: December 16, 1996[⊗]

A series of copolymer latices synthesized from pyrrole and *N*-methylpyrrole were prepared with similar particle sizes. After a detailed characterization of the particles the systems were prepared as electrorheological (ER) fluids in dodecane with the particles stabilized by a graft copolymer with poly(12-hydroxystearic acid) as the stabilizing moieties. The shear stress−shear rate behavior of the systems was studied over a shear rate range from 10^{-3} to 10^{3} s^{-1}. An ac electric field at 50 Hz was applied to the fluids using field strengths up to 1 kV mm^{-1} and the viscometric behavior examined. The particles with the highest conductivity exhibited Bingham behavior, and the fluid behavior could be calculated from the interparticle polarization forces. The Mason number provided good scaling of the data. The yield behavior was well described by the model due to Anderson and the high shear behavior by the Dougherty−Krieger equation. The fluids prepared with particles of lower conductivity showed pseudoplastic behavior with a power law index that was a function of conductivity, and the Mason number did not provide such a complete description of the viscometric response. The fluid with a particle conductivity of $\sim 10^{-9}$ S cm^{-1} showed no ER response.

1. Introduction

During the past decade there has been an increasing amount of interest in ER fluids[1] both theoretically and synthetically. An electrorheological fluid consists of a low conductivity oil phase with suspended particles which interact strongly, but reversibly, on the application of an electric field. Field strengths up to 3 or 4 kV mm^{-1} are commonly employed. In broad terms the requirements of a "good" electrorheological fluid are the following:

i. That there should be a marked change in rheological properties on the application of a field.

ii. The off-field viscosity should be close to that of the oil phase (i.e., the volume fraction, φ, should be < 0.3).

iii. The current requirement should be low to minimize power loss as well as heating effects.

iv. Low temperature sensitivity and hence water-free systems have an advantage.

v. There should be "tunability" of the particle properties to enable the maximum control of the ER properties as well as the suspension stability properties to be achieved.

vi. For comparison with theoretical models, monodisperse spherical particles would be the system of choice.

vii. There should be a strong effect in both dc and ac fields.

Water-free systems have been produced from polymeric particulates which have conducting properties.[2−4] Such systems have the advantage that the interfacial effects of the polarization of particles are minimized when compared to water-doped systems. The uniformity of the particles has been rather broad, however. The work reported here is a systematic study of the ER effect using monodisperse spherical particles of conducting polymer. By controlling the copolymerization, we were able to vary the particle conductivity over 7 orders of magnitude while achieving a similar particle size. The system chosen was a copolymer of pyrrole and *N*-methylpyrrole. Particle migration in ER fluids is a frequent experimental problem and is greatest at low applied fields and volume fractions. The systems used in the study responded to both ac and dc fields; however, throughout this study an ac field was utilized. This eliminated electrophoretic drift and so increased the reproducibility of the reported data.

2. Particle Synthesis and Characterization

2.i. Materials. Both the pyrrole and the *N*-methylpyrrole (Aldrich Chemicals) were distilled under reduced pressure and then stored under nitrogen at 4 °C prior to use. Ammonium persulfate (BDH Chemicals) and poly(ethylene oxide) (PEO) of $M_w = 3 \times 10^5$ (BDH Chemicals) were used as received. Water was purified using a Millipore "Milli Q" system.

2.ii. Latex Preparation. An aqueous solution of PEO was prepared at a concentration of 1.6 g dL^{-1} and was then added to an equal volume of ammonium persulfate solution at 4 °C. This mixture was allowed to equilibrate for 30 min at 4 °C, and then the monomers were added via a syringe pump to give a concentration of 1%. This reaction mixture was then stirred for a further 18 h to allow the polymerization to go to completion. A mole ratio of oxidant to monomer of 1.14:1 was used. An excess of oxidant is required to achieve oxidation of the polymer. Preparations up to 1 L in volume were prepared with a high degree of reproducibility.

The latices were dialyzed against water for at least 48 h with at minimum of 10 changes of dialyzate, to reduce the levels of any unreacted monomer and electrolytes to a low level. The PEO layer was removed from the surface of the particles by further washing[5] using eight cycles of centrifugation and decantation in methanol and a final wash using water. Redispersal of the particles between each cycle was achieved first by mechanical agitation and then by sonication. The pH was adjusted to ∼4 to ensure adequate charge stabilization of the particles as the isoelectric point of the particles was at pH 7 (see Figure 2).

2.iii. Particle Dispersal in Dodecane. Several steric stabilizers were examined as candidates for the formation of stable dispersions of the polymer particles in dodecane. The most effective stabilizer was a "comb" graft copolymer supplied by ICI, Paints Division, based on poly(12-hydroxy stearic acid) (PHS) grafted onto a poly(methyl methacrylate) backbone. This PHS stabilizer was received as a 40% solution in low boiling aliphatic hydrocarbon/ester solvent. Methanol was added to

[⊗] Abstract published in *Advance ACS Abstracts,* February 15, 1997.

S1089-5647(96)02267-5 CCC: $14.00

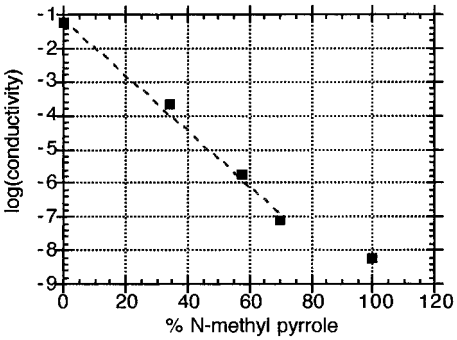

Figure 1. particle conductivity as a function of *N*-methylpyrrole content in the monomer feed.

precipitate the polymer. The precipitate was washed with methanol by 10 cycles of centrifugation and decantation. The precipitate was then dried under vacuum at 30 °C for 48 h. This temperature gave adequate drying of the polymer remaining well below the glass transition temperature (T_g) of the stabilizer (∼50−55 °C). Finally, the PHS was dissolved in dodecane to give a concentration of 2% w/w. Dissolution was achieved by stirring at a solution temperature of 80 °C for 2 h.

The polypyrrole copolymer particles were transferred from methanol to ethanol using three centrifugation/decantation cycles. The solution of PHS in dodecane was then added to the particles and redispersion was achieved with mechanical agitation followed by sonication. After allowing the system to equilibrate, the excess PHS stabilizer was removed using three centrifugation/decantation cycles.

2.iv. Particle Characterization. *Particle Size*. Transmission electron micrographs of the particles dried down from aqueous solution were obtained using a Jeol 100 CX Temscan microscope. A diffraction grating replica was photographed to provide a calibration. The mean particle size was obtained from measurement of at least 500 particles.

Conductivity. Conductivity measurements were performed on compressed pellets of the particles in order to characterize the properties of the polymer. Approximately 50 cm^3 of the dialyzed latices were freeze-dried overnight. These materials were then pelletized using an H30-1 pellet press, Research and Industrial Co., using a pressure of about 250 bar applied for 20 min. The conductivities of the pellets were measured with a Wayne-Kerr Universal bridge at a frequency of 1500 Hz. The full dielectric-frequency response was not investigated for these systems. For the lowest conductivity samples the pellets were coated with a gold layer on both top and bottom faces and then placed between two copper electrodes. For pellets with conductivities greater than 10^{-5} S cm^{-1} a four-in-line probe configuration was found to be satisfactory although gold coating was used for samples with conductivities up to 10^{-3} S cm^{-1}. For samples with conductivity between these values, good agreement was obtained between the two techniques. The results are shown in Figure 1. The addition of *N*-methylpyrrole to the monomer feed results in a marked reduction of the particle conductivity. The reduction has been reported by several authors[6−9] and is usually attributed to the twisting of the adjacent pyrrole rings relative to each other and so reducing the molecular orbital overlap.

Electrophoretic Mobility. The electrophoretic mobilities of the particles were measured using a PenKem System 3000. The latices were dispersed in 1×10^{-4} M potassium chloride and the pH was adjusted using dilute hydrochloric acid or sodium hydroxide solution, as appropriate. The polypyrrole particle concentration was <0.1%, and all solutions were filtered through a 0.2 μm filter prior to use. Some of the solutions were also

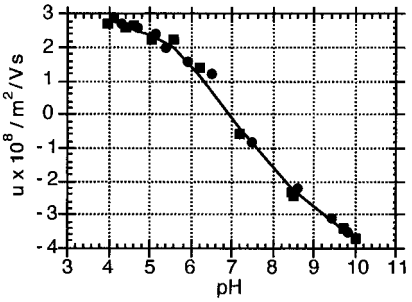

Figure 2. pH dependence of the electrophoretic mobility of systems (■) PER 45 and (●) PER 49 showing an isoelectric point at pH = 7 in both cases.

measured on a Brookhaven "Zetaplus" instrument, and good agreement was obtained between the two instruments. The data plotted in Figure 2 were typical of those found for all the latices, and all had isoelectric points in the range 6.5 < pH < 7.5. The mobility was also measured as a function of potassium chloride concentration at pH = 4.

Colloidal Stability. The critical coagulation concentration (c.c.c.) of the latices by potassium chloride solutions was determined at pH = 4. The experiments were carried out on latex dispersions with a particle concentration of 0.05% by adding varying amounts of a potassium chloride solution; a broad range of concentration was used initially in order to establish the region of rapid aggregation. This estimate was made by visual inspection of a set of tubes containing the latex/salt solutions after they had been allowed to equilibrate for 12 h. A narrower range of latex/salt solutions were prepared, and the rate of change of optical density with time was measured using a Kontron UV−visible spectrophotometer set at a wavelength of 500 nm. The optical density decreased with time due to the sedimentation of large aggregates. The electrolyte concentration giving the maximum rate was taken as the c.c.c.

The electrophoretic mobilities of the particles at the c.c.c. values were converted to ζ-potentials using the computer program of O'Brien and White,[10] and this enabled an estimate of the Hamaker constant, A_{11}, of the particles to be estimated. At the c.c.c. the maximum in the particle pair potential approaches zero and the force is also zero (see, for example, ref 11). An average value of $7.2 \pm 1 \times 10^{-20}$ J was calculated for the systems reported here. The value for water was taken as $A_{22} = 3.7 \times 10^{-20}$ J.[12] It is interesting to note that these values are lower than those reported for systems prepared with ferric chloride[13] by a factor of 3.5. However, the samples prepared with ferric chloride had a conductivity greater by 2 orders of magnitude.

Redispersion Check. The effectiveness of the redispersion of the particles into dodecane was checked by comparing the hydrodynamic diameters of the particles in dodecane with that found for the aqueous systems. Photon correlation spectroscopy was used to estimate the diffusion coefficient and hence yield a particle diameter. The data are shown in Table 1 and clearly illustrate the success in completely redispersing the particles. The hydrodynamic diameters are all slightly larger than those measured by TEM. This is usual with systems that use scattering as a detection system as greater weight is given to larger particles.

3. Viscometry

3.i. Apparatus. A Bohlin VOR Rheometer was used to measure the shear stress as a function of applied shear rate and ac electric field strength. The measuring geometry consisted of parallel stainless steel plates of 30 mm diameter mounted

TABLE 1: TEM Diameters, Particle Conductivity and Hydrodynamic Diameters, (d_h) of the Latices in Water and after Redispersal in Dodecane

				d_h/nm	
sample	% *N*-methylpyrrole in the feed	TEM diameter/nm	conductivity/S cm^{-1}	in water	in dodecane
PER 2	0	239 ± 20	5.80×10^{-2}	281	286
PER 45	34.1	227 ± 18	2.16×10^{-4}	254	258
PER 49	57.3	218 ± 17	1.87×10^{-6}	266	267
PER 48	70	232 ± 21	8.05×10^{-8}	258	262
PER 51	100	223 ± 22	6.20×10^{-9}	258	256

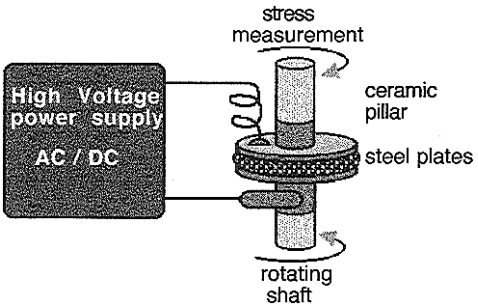

Figure 3. Schematic of the measuring geometry for the viscometry measurements.

on insulating ceramic pillars. The power supply was a Times Electronics Model 9822 unit which was set to operate at 50 Hz with voltages up to 1 kV. The electrical connections were via a running contact on the rotating element as shown in Figure 3. The upper element was permanently connected via a light coil in order to minimize contributions to the measured stress. The platen separation was 0.5 mm. This geometry provided a reasonably uniform electrical field, but the shear field varies with radius. Shear rates quoted are the average value (i.e., that found at ~0.66 of a radius from the center). The mean shear rate range investigated was from $10^{-3} < \dot{\gamma} < 10^{3}$ s^{-1}.

4. Results and Discussion

4.i. Preliminary Observations. All the samples except PER 51 showed an increase in viscosity when an electric field was applied. Sample PER 51 was the dispersion consisting of particles synthesized entirely from *N*-methylpyrrole, and the conductivity of the particles was low at 6.2×10^{-9} S m^{-1}. For the other dispersions, when the electric field was applied, the viscosity rose rapidly to its final value. The rise time appeared to be independent of applied field in the range $300 < E < 700$ V mm^{-1} as shown in Figure 4. On switching off the fields the viscosity dropped rapidly back to the zero-field value and there was no hysteresis. This was the case for all the ER fluid samples reported here. The use of an ac field limits particle migration, and the results clearly show that these systems are very responsive. Figure 5 also shows this response over the wide range of shear rates used.

Another noteworthy feature of the data in Figure 5 is that the power law is unity for PER 2. The simple form of the curves suggests that the data should be reasonably well fitted by the Bingham equation:

$$\sigma = \eta(\infty)\dot{\gamma} + \sigma_B; \quad \text{i.e., } \eta_a = \eta(\infty) + \sigma_B/\dot{\gamma} \qquad (1)$$

Here η_a is the apparent viscosity, $\eta(\infty)$ is the high shear limiting value (the plastic viscosity), and σ_B is the Bingham or dynamic yield stress.

The current density is an important parameter as the power requirement and heating effects can limit the application of ER fluids. Figure 6 shows data for three samples. All are low and indeed are much lower than those measured with polyaniline

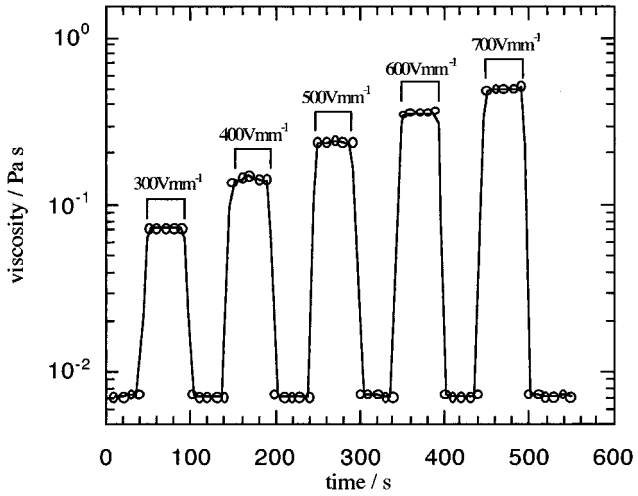

Figure 4. Periodic application of an ac electric field to sample PER 2 with increasing field strengths but with 30 s rest periods between applications. The shear rate was $\gamma = 10$ s^{-1} and the volume fraction of the sample was 0.187.

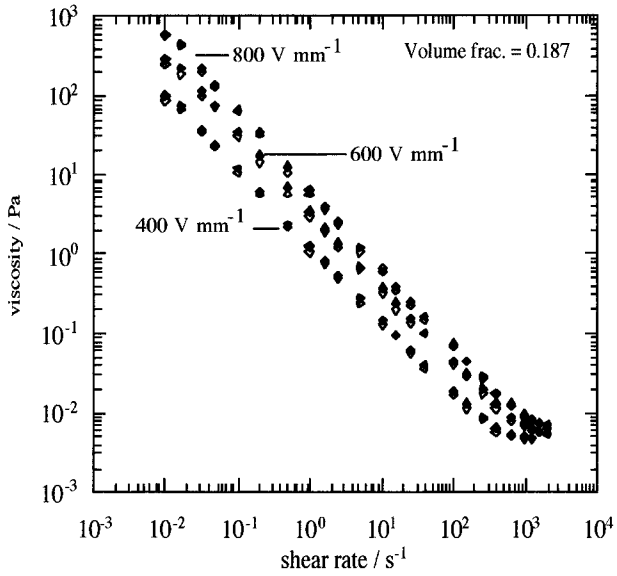

Figure 5. Viscosity of PER 2 at $\varphi = 0.187$ as a function of shear rate and applied field. Symbols: closed, increasing; open, decreasing shear rate.

fluids by Gow and Zukoski.[4] The polyaniline based systems were activated with hydrochloric acid while the systems studied in this work were prepared with persulfate. The values for PER 45 and PER 49 were similar throughout the range of field strengths. Both systems had large fractions of *N*-methylpyrrole in the preparations. PER 2 contained no *N*-methylpyrrole and the particles had the highest conductivity; however, the data in Figure 6 were for a system with substantially lower volume fraction than the other data and this resulted in a lower current density. When ferric chloride was used as an oxidant, much higher current densities were found with polypyrrole based systems also; i.e., chloride ion results in a more conducting fluid.

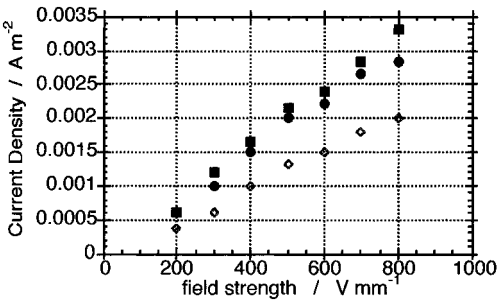

Figure 6. Current density as a function of applied field. (◇) PER 2 at $\varphi = 0.139$; (●) PER 49 at $\varphi = 0.178$; (■) PER 45 at $\varphi = 0.180$.

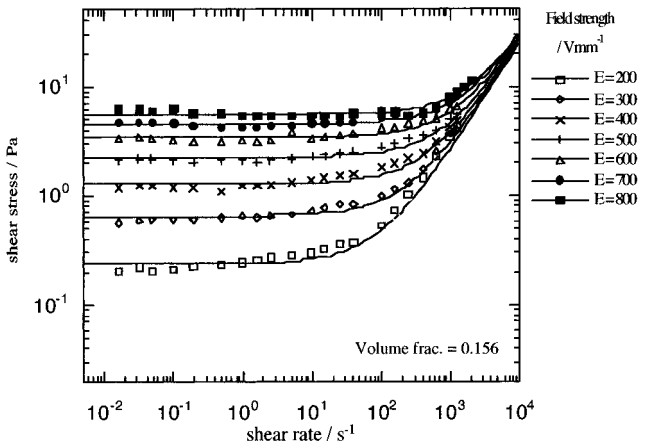

Figure 7. Shear stress as a function of shear rate for PER 2. Experimental points and calculated curve.

4.ii. Viscometric Results with PER 2. At high shear rates the viscosity of the suspensions approaches that of a simple sterically stabilized dispersion as the hydrodynamic forces dominate the interparticle forces. The high shear limiting viscosity can then be fitted to the Dougherty−Krieger equation:[14]

$$\frac{\eta(\infty)}{\eta_o} = \left(1 - \frac{\varphi}{\varphi_m}\right)^{-[\eta]\varphi_m} \tag{2a}$$

where η_o is the viscosity of dodecane (1.35×10^{-3} Pa s), the intrinsic viscosity $[\eta] = 2.5$, and the maximum packing $\varphi_m = 0.605$.[15]

Equation 1 combined with eq 2a then gives our constitutive equation for the fluid:

$$\sigma = \dot{\gamma}\eta_0\left(1 - \frac{\varphi}{\varphi_m}\right)^{-[\eta]\varphi_m} + \sigma_B \tag{2b}$$

Figure 7 illustrates the fit at $\varphi = 0.156$ with a range of applied fields. The Bingham (or in this case really the static) yield stress was the fitting parameter. Over the experimental range of shear rates, the Bingham model provides an adequate description of the experimental data. The dependence of the Bingham yield stress is shown in Figure 8. Good linear fits of the Bingham yield stress with volume fraction were obtained. The data were a function of applied electric field E so that

$$\sigma_B = kE^m \tag{3}$$

with $k \propto \varphi$. Figure 9 shows the value of m as a function of volume fraction. The dependence of the Bingham yield stress on field is E^2 at the higher volume fractions. The slightly higher values at lower volume fractions is probably an indication of a greater uncertainty in the fit of the shear stress−shear rate

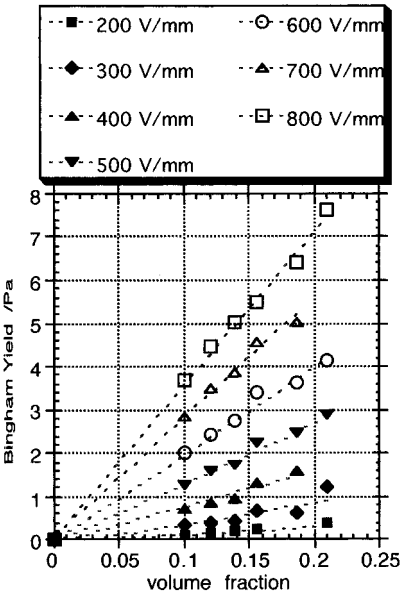

Figure 8. Bingham yield stress as a function of φ and E.

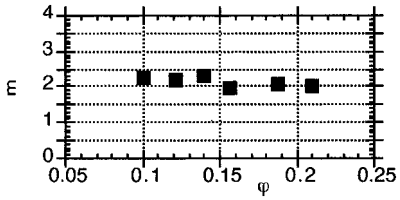

Figure 9. Field exponent m of the Bingham yield stress for PER 2.

curves. At low volume fractions and low field strengths there was a small decrease in stress (∼5%) at the lowest shear rates which gave rise to the increased uncertainty in the fit. As the ER effect becomes weaker, the existence of a static yield stress becomes more doubtful.

The change in viscosity with shear rate has been shown[16] to scale with the Mason number, Mn, which expresses the ratio between polarization forces and shear forces:

$$Mn = \frac{\eta_0\dot{\gamma}}{2\epsilon(\beta E)^2} \tag{4}$$

where ϵ is the permittivity of the oil phase and β is a function of the permittivities both the particles and the oil:

$$\beta = \left(\frac{\epsilon_p - \epsilon}{\epsilon_p + 2\epsilon}\right) \approx 1 \qquad \text{for the system used here}$$

In addition, the critical Mason number, Mn^*, is defined[16] as the intersection of the linear fall of the log(relative viscosity) versus log(Mn) with the horizontal line representing the high shear viscosity plateau. Figure 10 shows a typical plot. The experimental data gave a value of the $Mn^* \sim 0.1$ as shown in Figure 11. Thus the following relationship should collapse all the data onto a master curve:

$$\frac{\eta}{\eta(\infty)} = 1 + \frac{Mn^*}{Mn} \tag{5}$$

This is shown in Figure 12 for all the data obtained on sample PER 2. All the data fit closely to a single line illustrating how effective this scaling is with this system which has the highest particle conductivity. It should be remembered, however, that in deducing the form of eq 5, the Bingham equation was used as the constitutive equation for the fluid. If this were not an

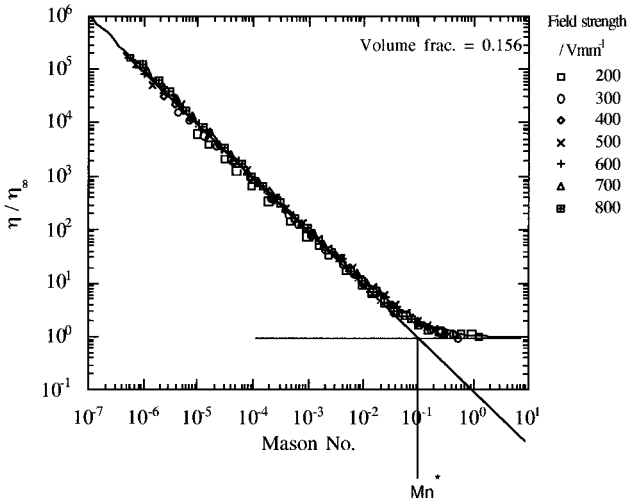

Figure 10. Determination of the critical Mason number for PER 2 at $\varphi = 0.156$ showing data at all applied field strengths.

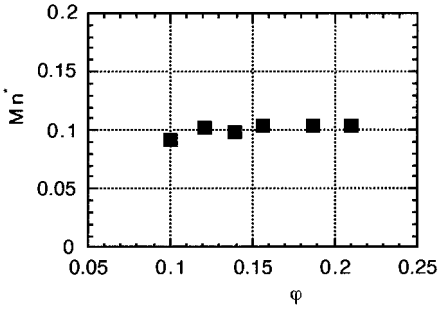

Figure 11. Mason number as a function of volume fraction.

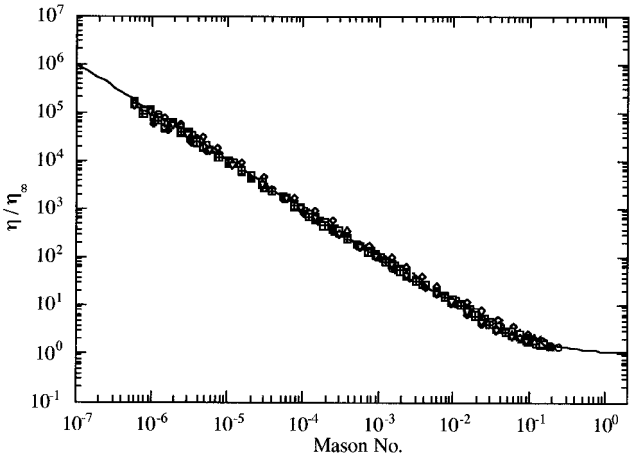

Figure 12. Viscosity relative to the high shear limit for all volume fractions at all applied fields for sample PER 2.

adequate fit to the experimental behavior, which would be the case if the fluids were pseudoplastic, eq 5 would not produce such a good master curve.

4.iii. Particle Conductivity and the Viscometric Response. As the conductivity of the particles is reduced, the strength of the ER response was observed to decrease. This was not a very marked effect, but a more significant change which was observed was the change from plastic to psuedoplastic behavior as the conductivity decreased. This means that the simple and convenient Bingham constitutive equation is no longer an adequate descriptor of the viscometric response. The loss of a true or static yield stress and the introduction of a zero shear viscosity should be more easily observed at lower applied electric field strengths. Figure 13 shows an example of the observed response for one of the fluids with low conductivity

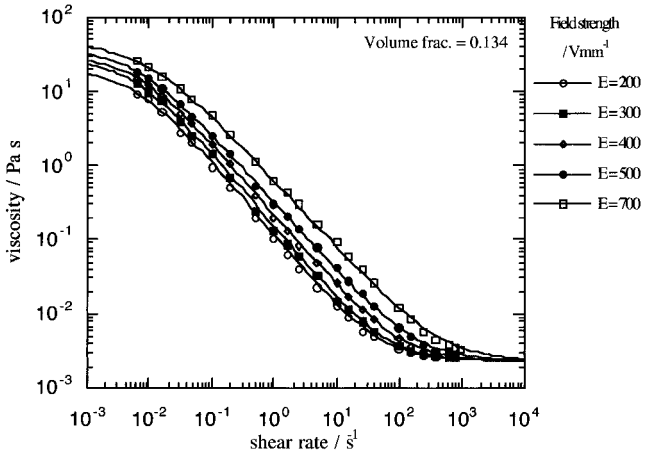

Figure 13. Viscosity as a function of shear rate for PER 48 at $\varphi = 0.134$ with a particle conductivity of 8.05×10^{-8} S cm^{-1}.

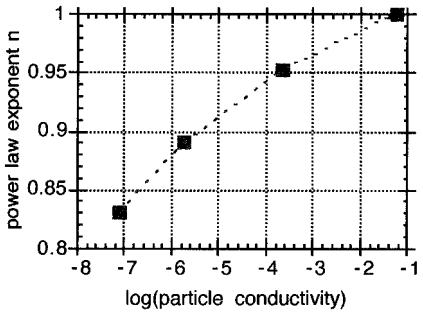

Figure 14. Power law exponent as a function of conductivity.

particles: PER 48. In this case, although increasing applied electric field increases the viscosity, all the plots show curvature at $\dot{\gamma} < 0.1$ s^{-1}. The zero shear viscosity, $\eta(0)$, would not be achieved until $\dot{\gamma}$ values as low as 10^{-4} s^{-1} had been achieved. At high shear rates there is a convergence of all the curves at the different field strengths to the high shear limiting viscosity, as would be expected. The Cross equation[17] gives a good fit to the experimental data:

$$\eta = \eta(\infty) + \frac{\eta(0) - \eta(\infty)}{1 + C\dot{\gamma}^n} \qquad (6)$$

Here C and n are material parameters. Cross argued that $n \sim 1$ for monodisperse systems and decreased to 2/3 with increasing polydispersity. The high shear limiting viscosity was obtained from eq 2a, and the low shear limiting values were given as the best fits. There were no data available at shear rates below 10^{-3} s^{-1} to obtain experimental values. The values of the power law exponent, n, found for the ER fluids are plotted in Figure 14. The values agree well with the two-dimensional simulations of Baxter-Drayton and Brady[19] covering a similar shear rate range and are close to those of Halsey et al.[18] using higher shear rates with silica particles with a larger particle size than the systems used in this work. It is interesting to note that there is a decrease with decreasing particle conductivity and hence with increasing pseudoplastic behavior.

Although there is not static yield response, the zero shear viscosity will reflect the strength of the particle interactions in the fluids, and this is reflected in Figure 13. However, numerical values cannot be quoted here as lower values of shear rate would have to have been probed. The values obtained by fitting eq 6 will have too great an uncertainty to warrant further analysis.

It is interesting to examine the effectiveness of the scaling of these pseudoplastic materials using the Mason number. This

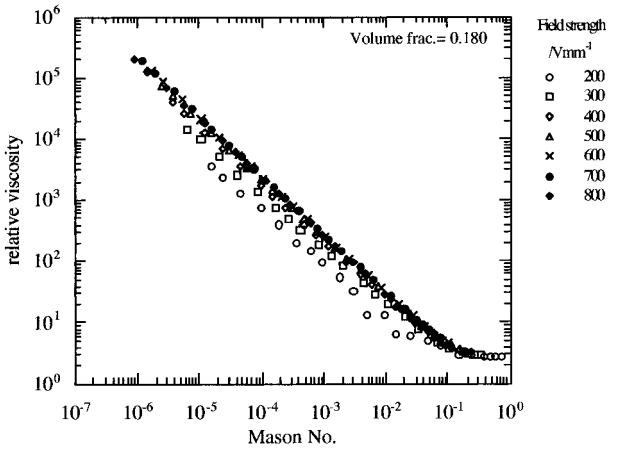

Figure 15. Viscosity versus Mason number for PER 45 at $\varphi = 0.18$.

is illustrated by Figure 15 for the data for PER 45 which showed only a slight indication of pseudoplasticity, but a rather poorer scaling of the applied field response for values of $E < 400$ V mm^{-1}. Here the power law index varies from 0.86 at $E = 200$ V mm^{-1} to 0.94 at $E = 400$ V mm^{-1}.

Just as the Mason number is the ratio of the viscous to polarization forces, the Peclet number gives the ratio of the viscous to the Brownian or thermal forces:

$$Pe = \frac{6\pi\eta_0 a^3 \dot{\gamma}}{kT} \tag{7}$$

The ratio of the Peclet number to the Mason number defines the ratio of the polarization to Brownian forces: λ. The field strength range of 100 V mm^{-1} < E < 800 V mm^{-1} gives a range of $2.8 < \lambda < 176$. Baxter-Drayton and Brady[19] showed that shear thinning could be expected at shear rates in excess of

$$\dot{\gamma} > \frac{6\pi\eta_0 a^3}{kT}\lambda e^{-\lambda} \tag{8}$$

and this corresponds to Mason numbers of 1×10^{-7}, 3×10^{-8}, and 6×10^{-9} for fields of 200, 300, and 400, respectively. In order to explore this region with for example the system illustrated in Figure 14, a different experimental setup would be required, preferably based on the controlled stress rheometer as opposed to the controlled strain instrument.

4.iv. The Yield Stress. Several authors have attempted to model the yield behavior of ER fluids. Both analytic and computer modeling have been carried out. Here we will compare the results of the analytic models of Klingenberg and Zukoski[20] with that of Anderson.[21] The system we shall use is PER 2 as it showed the simplest response and could be well described by the Bingham constitutive equation and hence we do not need to distinguish between static and dynamic yield processes.

Many workers have shown how linearized structures are observed in dilute ER fluids parallel to the applied field direction. At higher concentrations this is more difficult to observe optically but the structural organization of the particles is a key starting point for calculation. The other key parameter is the pair potential due to the applied field. If we consider the pair interaction to be due to the rapid polarization of the particles in the applied ac field, then the force per pair interaction is given by[16]

$$F = \epsilon(a\beta E)^2 f \tag{9}$$

where f is a geometric factor and for our systems $\beta \sim 1$.

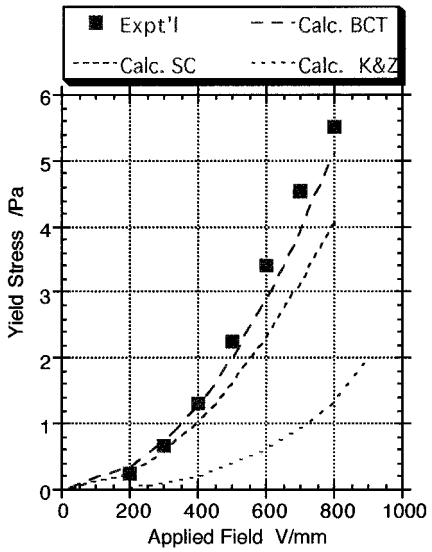

Figure 16. Yield stress for PER 2 at $\varphi = 0.156$. SC is simple cubic structure, BCT is body-centered tetragonal structure, and K & Z is the method for simple strings from Klingenberg and Zukoski.

Klingenberg and Zukoski[20] modeled the yield process with a model of discrete particulate strings being stretched to a critical extension and breaking, followed by the joining of adjacent strings. Anderson[21] took into account the more complex structure that could be expected at moderate particle concentrations and modeled the process from the starting point of columns of particles. As the boundaries of the fluid are moved the columns are stretched. In order to maintain particles in close proximity, the columns were considered to become narrower. This approach requires a local structural model in order to give a detailed description of the interactions in the columns. The force within a chain, F_c, is

$$F_c = \pi\epsilon E^2 a^2 \beta^2 [\delta_r^{-1} - 2(1 + \delta_r)\ln(\delta_r^{-1} + 1) + 2] \tag{10}$$

with $\beta \sim 1$, δ_r, the minimum surface separation relative to the particle diameter, and the systems used here resulted in a value of $\delta_r \sim 0.07$. The stress required to break a column is then given by the product of this force and the areal density of chains, A_c. When a shear strain was applied, the columns were considered to become narrower (i.e., the volume of the columns were conserved in contrast to the Klingenberg and Zukoski model where the particle separation increased), giving a maximum stress at an angle θ and giving rise to an additional geometric factor of $\cos^3\theta \sin\theta$ and hence

$$\sigma_B \cong \sigma_y = F_c A_c \cos^3\theta \sin\theta \tag{11}$$

A simple cubic arrangement could be assumed, for example, but a body-centered tetragonal structure has been identified from calculation.[22,23] The equivalence of the static yield, σ_y, to the dynamic yield is due to the use of the Bingham constitutive equation. The best fit is from the model of Anderson with a body-centered tetragonal structure, and it provides a good description of the yield. The fits are shown in Figure 16.

5. Conclusions

Monodisperse, spherical, conducting polymer latices have provided good model systems for ER fluid studies. The highest conductivity systems showed the strongest effect with a Bingham body response. The yield behavior of the system was well described by the model due to Anderson using a body-centered

tetragonal local structure. With the high shear viscosity being given by the Dougherty−Krieger equation, the full shear stress−shear rate behavior could be predicted. The use of the Mason number enabled all the data to be collapsed onto a single curve illustrating how the polarization forces in the ac applied field provide an excellent description of the ER effect.

With this model system, as the particle conductivity decreased the effect was found to weaken but, more importantly, the systems became increasingly pseudoplastic and the power law index was observed to decrease systematically. The Mason number plots were less successful in providing a master curve.

References and Notes

(1) Gast, A.; Zukoski, C. F. *Adv. Colloid Interface Sci*. **1989**, *30*, 153.
(2) Block, H.; Kelly, J. P.; Qin, A.; Watson, T. *Langmuir* **1990**, *30*, 6.
(3) Filisko, F. E.; Radzilowski, L. H. *J. Rheol*. **1990**, *34*, 539.
(4) Gow, C.; Zukoski, C. F. *J. Colloid Interface Sci*. **1990**,*136*, 175.
(5) Cawdrey, N.; Obey, T. M.; Vincent, B. *J. Chem. Soc., Chem. Commun.* **1988**, 1189.
(6) Kanazawa, K. K.; Diaz, A. F.; Krounbi, M. T.; Street, G. B. *Synth. Met*. **1981**, *4*, 119.
(7) Reynolds, J. R.; Poropatic, P. A.; Toyooka, R. L. *Macromolecules* **1987**, *20*, 958.
(8) Neoh, K. G.; Kang, E. T.; Tan, T. C.; Tan, K. L. *J. Appl. Polym. Sci.* **1989**, *38*, 2009.
(9) Kiana, M. S.; Mitchell, G. R. *Synth. Met*. **1992**, *46*, 293.
(10) O'Brien, R. W.; White, L. R. *J. Chem Soc., Faraday Trans. 2* **1987**, *74*, 1607.
(11) Hunter, R. J. *The Foundations of Colloid Science*; Vols I & II; Oxford University Press: Oxford, 1989.
(12) Israelachvili, J. *Intermolecular and Surface Forces*; Academic Press: London, 1985.
(13) Markham, G. M.; Obey, T. M.; Vincent, B. *Coll. Surf.* **1990**, *51*, 239.
(14) Krieger, I. M. *Adv Colloid Interface Sci*. **1972**, *3*, 111.
(15) Goodwin, J. W.; Ottewill, R. H. *J. Chem Soc., Faraday Trans. 1* **1991**, *87*, 357.
(16) Goodwin, J. W.; Marshall, L.; Zukoski, C. F. *J. Chem. Soc., Faraday Trans. 1* **1989**, *85*, 2785.
(17) Cross, M. M. *J. Colloid Sci*. **1965**, *20*, 147.
(18) Halsey, T. C.; Martin, J. E.; Adolf, D. *Phys. Rev. Lett*. **1992**, *68*, 1519.
(19) Baxter-Drayton, Y.; Brady, J. F. *J. Rheol*. **1996**, *40*, 1027.
(20) Klingenberg, D. J.; Zukoski, C. F. *Langmuir* **1990**, *6*, 15.
(21) Anderson, R. A. *Langmuir* **1994**, *10*, 2917.
(22) Tao, R.; Sun, J. M. *Phys. Rev. Lett.* **1991**, *67*, 398.
(23) Tao, R. *Phys. Rev. E* **1993**, *47*, 423.